Brillouin propagation modes of cold atoms undergoing Sisyphus cooling

David Cubero ⬤*

Departamento de Física Aplicada I, Escuela Politécnica Superior, Universidad de Sevilla, Calle Virgen de África 7, 41011 Sevilla, Spain

An exact expression for the average velocity of cold atoms in a driven, dissipative optical lattice in terms of the amplitudes of atomic density waves is derived from semiclassical equations for the phase space densities of the Zeeman ground-state sublevels. The calculations are for a $J_g = 1/2 \to J_e = 3/2$ transition, as it is customary in theoretical studies of Sisyphus cooling. While the driver, an additional beam of small amplitude, sets the atoms into directed motion, the new expression permits the quantification of the contribution to the atomic motion of a specific atomic wave, revealing unexpected counterpropagating contributions from many modes. Additionally, the method is shown to provide the generic threshold for the transition into the regime of infinite density, regardless of the details, or even the presence, of driving.

I. INTRODUCTION

Laser cooling of atoms to very low temperatures [1] has been a crucial experimental achievement in atomic, molecular, and condensed matter physics. Several Nobel Prizes have been awarded for the development of techniques in this subject. Among them, Sisyphus cooling [2] is widely used to cool atoms below the Doppler temperature limit.

Cold atoms offer an invaluable setup to study directed transport, and many experimental realizations of dissipative, Sisyphus cooling based [3–8], and nondissipative [9,10] ratchets [11,12] have been demonstrated on them. They provide quantum ratchets [12] with a high degree of tunability, complementing other known quantum setups [13–16].

Additionally, cold atoms are also known to exhibit unusual transport behavior beyond Boltzmann-Gibbs statistical mechanics [17], usually referred as a regime of infinite density [18–21] in which the probability distributions are non-normalizable due to the broken ergodicity.

This paper is focused in cold atoms in laser setups associated with Sisyphus cooling. They are created by counterpropagating laser beams that can be tuned experimentally with a high level of control. The system is theoretically analyzed at the level of semiclassical equations for the atomic phase-space densities [22]. The study is restricted to atoms with a transition $J_g = 1/2 \to J_e = 3/2$, as it is customary in the theoretical analysis of Sisyphus cooling [2] because it exhibits the essential ingredients observed in atoms with more complex atomic transitions when the optical potential wells are not too deep [22]. It is worth mentioning, though, that the method proposed here could be lengthy, but straightforwardly applied to the semiclassical equations of atoms with more complex transitions.

Special attention is paid to atomic transport. A perturbing probe beam is introduced [2,23–25] to break the system symmetries [12,26] and put the atoms into directed motion. The probe perturbation excites atomic density waves, which are referred to as Brillouin propagating modes [24,25] due to the resemblance to acoustic waves rippling through a dense fluid.

Previous research mostly focused on one propagating mode, the one with same frequency and wave number as the propagating perturbation, ignoring the effect of other excited modes, propagating or not. Here, we address this issue by deriving an exact expression for the current as a sum of terms proportional to the amplitudes of the excited atomic density waves. Since other modes are observed to contribute significantly to the directed motion, as demonstrated in Sec. IV, the derived expression can provide a useful tool in order to properly rationalize the dynamical properties of the ratchet system.

Additionally, the summation directly reveals a singularity that is identified with the threshold to the regime of infinity density. The threshold values are in agreement with previous analytical results [18,19] obtained from a simplified, approximate Fokker-Planck equation [27] based on space and Zeeman sublevel averaging of the semiclassical equations, thus with drastic approximations whose validity is difficult to evaluate. The method presented here does not make such approximations, being based on the semiclassical equations it takes explicitly into account the microscopic origin of Sisyphus cooling, thus providing desirable support for previous results [18,19] on infinity densities.

The paper is organized as follows. In Sec. II the system models studied are described. A new method, relating the current and higher moments to atomic density modes, is presented in Sec. III. The application of the method to the system, its analytical results and numerical validation, is described in Sec. IV. The transition to the regime of infinity density, coming out naturally from a singularity in the analytical results, is discussed in Sec. V. Finally, Sec. VI summarizes the main conclusions.

II. SYSTEM MODELS

First, we consider the simplest model of dissipative Sisyphus cooling, a one-dimensional (1D) system gener-

----

*dcubero@us.es

ated by atoms with a closed transition $J_g = 1/2 \rightarrow J_e = 3/2$, mass m_a, illuminated by two counterpropagating laser fields with orthogonal linear polarizations. This setup generates a 1D optical lattice in the light polarization so-called lin $\perp$ lin configuration [2]. The atom, in the Zeeman sublevel of the atomic ground state $|J_g = 1/2, M_g = +1/2\rangle$ or $|J_g = 1/2, M_g = -1/2\rangle$, which for convenience we abbreviate to $+$ or $-$, respectively, experiences the optical potential

$$U_\pm(x) = \frac{U_0}{2}[-2 \pm \cos(2k_l x)], \qquad (1)$$

where x is the laser beam propagation axis, k_l the laser field wave vector, and U_0 the optical lattice depth.

In the semiclassical approximation for weak laser intensities, the atoms in the ground state $|\pm\rangle$ satisfy [22] the following coupled Fokker-Planck equations for the phase space density $P_\pm(x, p, t)$ at the position x with momentum p:

$$\left[\frac{\partial}{\partial t} + \frac{p}{m_a}\frac{\partial}{\partial x} - U'_\pm(x)\frac{\partial}{\partial p} + F_\pm(x, t)\frac{\partial}{\partial p}\right]P_\pm$$

$$= -\gamma_\pm(x)P_\pm + \gamma_\mp(x)P_\mp + \frac{\partial^2}{\partial p^2}[D_0 P_\pm], \qquad (2)$$

where $U'_\pm = \partial U_\pm/\partial x$, $\gamma_\pm(x)$ are the transition rates between the ground-state sublevels, D_0 is a noise strength describing the random momentum jumps that result from the interaction with the photons, and $F_\pm(x, t)$ are nonconservative forces, coming, for example, from radiation pressure, or an arbitrary time-dependent driving force $F(t)$ that can be generated by phase modulating one of the lattice beams [28].

Equation (2) is complemented by the normalization condition,

$$\int dx \int dp[P_-(x, p, t) + P_+(x, p, t)] = 1. \qquad (3)$$

A quantity of special interest is the average atomic current, which measures the directed motion, defined as

$$\langle v \rangle = \lim_{t \to \infty} \frac{\langle [x(t) - x(0)]\rangle}{t}$$

$$= \lim_{t \to \infty} \frac{1}{t}\int_0^t dt' \int dx \int dp \frac{p}{m_a}$$

$$\times [P_+(x, p, t') + P_-(x, p, t')]. \qquad (4)$$

A. 1D lin $\perp$ lin setup

In the 1D lin $\perp$ lin configuration without driving there is no radiation pressure, i.e., $F_\pm(x, t) = 0$, and

$$U_0 = -2\hbar\Delta'/3 > 0, \qquad (5)$$

where Δ' is the light shift per beam for our closed $J_g = 1/2 \rightarrow J_e = 3/2$ transition. Furthermore, the transition rates between the internal states are given by

$$\gamma_\pm(x) = g_0 \pm g_1 \cos(k_0 x), \qquad (6)$$

where $k_0 = 2k_l$, $g_0 = \Gamma'/9$, and $g_1 = g_0$ are rates related to the photon scattering rate per lattice beam Γ'.

Note that in writing (2) we are not explicitly considering an extra diffusive term that comes up in the semiclassical approximation [22], $\partial^2 D_{\mp\pm}P_\mp/\partial p^2$, which describes a further

momentum kick when the transitions take place, and needs to be corrected to avoid artificial numerical singularities, in the form of divergent momentum, produced by the semiclassical approximation, as discussed in Ref. [19]. When corrected, the effect of that term is nevertheless small, and commonly neglected, unless shallow optical potentials are considered [19]; more about this issue in Sec. V.

In addition, we are not explicitly considering any state or spatial dependence of the noise coefficient D_0, because their effect is observed to be small in the simulation results reported in this paper. Neglecting $D_{\mp\pm}$ and taking the space average of the remaining diffusion coefficient in the original semiclassical equations [22] yields $D_0 = 35\hbar^2 k_l^2 \Gamma'/90$.

The application of an additional weak probe beam generically produces extra small contributions to all the functions: the optical potential, radiation pressure forces, transition rates, and noise terms, though the most relevant contribution is the one in the optical potential. Numerical simulations show that the contributions from the former terms are usually small, not altering the qualitative picture offered by a model with a probe potential addition. We consider here a probe beam that is polarized parallel to the 1D counterpropagating lattice beam, which yields the optical potential

$$U_\pm(x, t) = \frac{U_0}{2}[-2 \pm \cos(k_0 x) + \varepsilon_p \cos(k_0 x - \delta_p t + \phi_p)], \qquad (7)$$

where, for the 1D setup, $\varepsilon_p = 2E_p/E_0$ is defined as twice the ratio between the electric field of the probe E_p to that of the underlying optical lattice E_0, $\delta_p = \omega_p - \omega_l$ is the probe frequency detuning, with ω_p the probe frequency and ω_l the lattice beam frequency, and ϕ_p is the probe phase.

B. 3D lin $\perp$ lin setup

In addition to the above 1D lin $\perp$ lin configuration, we will study the one-dimensional system that arises in the standard 3D lin $\perp$ lin configuration [2], after neglecting movement in the two directions perpendicular to the direction of interest, usually taken as the x axis [23,24,29–31]. weak y-polarized probe propagating in the z direction is added [24,25,31], yielding in the optical potential an extra term proportional to

$$\cos(k_x x)\cos(\delta t) = \tfrac{1}{2}[\cos(-k_x x - \delta_p t) + \cos(+k_x x - \delta_p t)], \qquad (8)$$

where $k_x = k_l \sin\theta_x$, thus being the superposition of two sinusoidal potentials traveling in the x direction, each with opposite velocity and similar shape as in the previous 1D system model. By formally considering $y = z = 0$ and one of the traveling probe drives, the optical potential in each sublevel of the ground state is given by [2,31]

$$U_\pm(x, t) = \frac{U_0}{2}\left[-\frac{3}{2} - \frac{1}{2}\cos(2k_0 x) \pm \cos(k_0 x)\right.$$

$$\left. + \varepsilon_p \cos(k_0 x - \delta_p t + \phi_p)\right], \qquad (9)$$

with transition rates given by

$$\gamma_\pm(x) = g_0 \pm g_1 \cos(k_0 x) + g_2 \cos(2k_0 x), \qquad (10)$$

where now $k_0 = k_x$, $U_0 = -16\hbar\Delta_0'/3$, $\Delta_0'(< 0)$ is the light shift per lattice field, $g_0 = 2\Gamma'/3$, $g_1 = 8\Gamma'/9$, $g_2 = 2\Gamma'/9$, and now $\varepsilon_p = E_p/(2E_0)$ for the 3D setup. Like before, for the sake of simplicity, we are neglecting the probe contribution to the transition rates, the radiation forces, and noise terms, being observed their effect to be small in the simulations. Finally, the noise strength is $D_0 = 5\hbar^2 k_0^2 \Gamma'/18$.

III. FOURIER MODE THEORY

We develop in this section a theory that will allow us to visualize the atomic density modes excited by the probe and their contribution to the current. First, the atomic Fourier modes are defined from the phase-space density $P_\pm(z, p, t)$ by means of the following Fourier transform:

$$\mathcal{P}_{\omega,k,q}^\pm = \frac{1}{T_p} \int_0^{T_p} dt\, e^{-i\omega t} \int dx\, e^{ikx} \int dp\, e^{ipq/\hbar} P_\pm(x, p, t), \tag{11}$$

where $T_p = 2\pi/\delta_p$ is the time period introduced by the probe, ω and k are a frequency and a wave number, respectively, associated with the time and space Fourier transform, and q is an extra Fourier coordinate needed to account for the atomic momentum. The fact that the driving probe is time periodic allows us to focus on solutions, which have the same periodicity, i.e., to

$$\omega = l\delta_p, \tag{12}$$

with l integer, thus neglecting transitory dependencies on a specific initial condition, which are expected to die out after a transient time interval (involving necessarily many atomic transitions for Sisyphus dissipation to take place). In addition, the fact that the phase-space densities are real implies

$$\mathcal{P}_{-\omega,-k,-q}^\pm = (\mathcal{P}_{\omega,k,q}^\pm)^*, \tag{13}$$

where $*$ denotes complex conjugate.

Now, let us consider a generic 1D setup determined by (2) and (3), with a periodic optical potential

$$U_\pm(x + 2\pi/k_0) = U_\pm(x), \tag{14}$$

and space periodic transition rates,

$$\gamma_\pm(x + 2\pi/k_0) = \gamma_\pm(x), \tag{15}$$

and time and space periodic driving,

$$F_\pm(x + 2\pi/k_0, t) = F_\pm(x, t + 2\pi/\delta_p) = F_\pm(x, t), \tag{16}$$

for all x, t.

Using (11), the Fokker-Planck Eq. (2) is transformed into

$$i\omega \mathcal{P}_{\omega,k,q}^\pm - \frac{\hbar k}{m_a} \frac{\partial}{\partial q} \mathcal{P}_{\omega,k,q}^\pm$$
$$- \frac{iq}{\hbar} \left(\sum_n \mathcal{F}_n^{(0)\pm} \mathcal{P}_{\omega,k-nk_0,q}^\pm + \sum_{l,m} \mathcal{F}_{l,m}^{p\pm} \mathcal{P}_{\omega-l\delta_p,k-mk_0,q}^\pm \right)$$
$$= -\sum_n (\gamma_n^\pm \mathcal{P}_{\omega,k-nk_0,q}^\pm - \gamma_n^\mp \mathcal{P}_{\omega,k-nk_0,q}^\mp) - \frac{q^2}{\hbar^2} D_0 \mathcal{P}_{\omega,k,q}^\pm, \tag{17}$$

where we have taken advantage of the periodicity, allowing us to write

$$-\frac{\partial U_\pm}{\partial x} = \sum_n \mathcal{F}_n^{(0)\pm} e^{-ink_0 z}, \tag{18}$$

$$F_\pm(z, t) = \sum_{l,m} \mathcal{F}_{l,m}^{p\pm} e^{-i(mk_0 z - l\delta_p t)}, \tag{19}$$

and

$$\gamma_\pm(z) = \sum_n \gamma_n^\pm e^{-ink_0 z}. \tag{20}$$

In the problems considered here, there is no force bias, i.e.,

$$\mathcal{F}_0^{(0)\pm} = \mathcal{F}_{0,0}^{p\pm} = 0, \tag{21}$$

and the states are symmetric:

$$\gamma_0^\pm = \gamma_0. \tag{22}$$

From (11), the application of the normalization condition (3) yields

$$\mathcal{P}_{l\delta_p,0,0}^+ + \mathcal{P}_{l\delta_p,0,0}^- = \frac{1}{T_p} \int_0^{T_p} dt \exp[-il\delta_p t], \tag{23}$$

thus,

$$\mathcal{P}_{l\delta_p,0,0}^- = -\mathcal{P}_{l\delta_p,0,0}^+ \quad \text{for } l \neq 0, \quad \text{and} \tag{24}$$

$$\mathcal{P}_{0,0,0}^+ + \mathcal{P}_{0,0,0}^- = 1. \tag{25}$$

Once $\mathcal{P}_{\omega,k,q}^\pm$ is known, the phase-space density is retrieved back by means of the inverse transform,

$$P_\pm(x, p, t) = \frac{1}{4\pi^2\hbar} \sum_l \int dk \int dq\, e^{-i(kx - tl\delta_p)} e^{-ipq/\hbar} \mathcal{P}_{l\delta_p,k,q}^\pm. \tag{26}$$

We are specially interested in the marginal probability $P_\pm(x, t) = \int dp\, P_\pm(x, p, t)$, which can be obtained from $\mathcal{P}_{\omega,k,q}^\pm$ with $q = 0$,

$$P_\pm(x, t) = \frac{1}{2\pi} \sum_l \int dk\, \mathcal{P}_{l\delta_p,k,0}^\pm e^{-i(kx - tl\delta_p)}. \tag{27}$$

The normalization condition (25) and the equations of motion (17) only requires excitation of a discrete set of wave number values

$$k = nk_0 \tag{28}$$

where n is an integer.

Note Eq. (27) expresses the atomic density as a sum of plane waves, atomic density modes, each moving with velocity $(l/n)\delta_p/k_0$. The case $(l, n) = (1, 1)$ has been explicitly referred to as a Brillouin-like propagation mode [2,23,24], because of the analogy with the resonances produced by light scattering on propagative modes in fluids, such as sound waves.

Assuming, like in (11), that at time $t = 0$ all the transients have already died out, the atomic current (4) can be written in

terms of the mode amplitudes as

$$
\begin{aligned}
\langle v \rangle &= \frac{\delta_p}{2\pi} \int_0^{2\pi/\delta_p} dt \int dx \int dp \, \frac{p}{m_a} \\
&\quad \times [P_+(x, p, t) + P_-(x, p, t)] \\
&= \lim_{q \to 0} \frac{\hbar \delta_p}{i m_a 2\pi} \frac{\partial}{\partial q} \int_0^{2\pi/\delta_p} dt \int dx \int dp \, e^{i(kx - \omega t + pq/\hbar)} \\
&\quad \times [P_+(x, p, t) + P_-(z, p, t)] \big|_{\omega = k = 0} \\
&= \frac{\hbar}{i m_a} \lim_{q \to 0} \left(\frac{\partial \mathcal{P}_{0,0,q}^+}{\partial q} + \frac{\partial \mathcal{P}_{0,0,q}^-}{\partial q} \right).
\end{aligned} \tag{29}
$$

The equations (17) and (25) can be used to find $\partial \mathcal{P}_{0,0,0}^\pm / \partial q$ in terms of the mode amplitudes $\mathcal{P}_{\omega,k,0}^\pm$, thus providing the exact contribution of each excited mode to the atomic current, yielding one of the central analytical results of this paper, in which the current (4) is written as

$$
\langle v \rangle = \sum_{l,n} v[l, n] = \sum_{l,n} v_{l,n}^+ \mathcal{P}_{l\delta_p, nk_0, 0}^+ + v_{l,n}^- \mathcal{P}_{l\delta_p, nk_0, 0}^-, \tag{30}
$$

with explicit analytical expressions for the coefficients $v_{l,n}^\pm$ for the specific system at hand, as reported in Sec. IV.

The same procedure can be applied to compute any moment of the velocity distribution, $\langle v^n \rangle$, with n a positive integer, since following similar steps as in (29) one easily obtains

$$
\langle v^n \rangle = \left(\frac{\hbar}{i m_a} \right)^n \lim_{q \to 0} \left(\frac{\partial^n \mathcal{P}_{0,0,q}^+}{\partial q^n} + \frac{\partial^n \mathcal{P}_{0,0,q}^-}{\partial q^n} \right), \tag{31}
$$

with q derivatives that can be found in terms of the amplitudes of the atomic waves in a similar fashion as before.

A. Basic symmetry

Due to the vectorial nature of both the driving force $F_\pm(x, t)$ and the current $\langle v \rangle$, the inversion transformation $x \to -x$ yields an inverted current [32], a fact which is behind the (easy to verify) statement that the solution of the problem with conservative force

$$
\widehat{\mathcal{F}}_n^{(0)\pm} = -\mathcal{F}_{-n}^{(0)\pm}, \tag{32}
$$

and driving force

$$
\widehat{\mathcal{F}}_{l,m}^{p\pm} = -\mathcal{F}_{l,-m}^{p\pm}, \tag{33}
$$

is just

$$
\widehat{\mathcal{P}}_{\omega,k,q}^\pm = \mathcal{P}_{\omega,-k,-q}^\pm, \tag{34}
$$

which, by virtue of (29), yields

$$
\langle \widehat{v} \rangle = -\langle v \rangle. \tag{35}
$$

Note if the potential is spatially symmetric, then

$$
\mathcal{F}_n^{(0)\pm} = -\mathcal{F}_{-n}^{(0)\pm}, \tag{36}
$$

and to produce a current we need a symmetry-breaking probe.

B. Sketch of the calculation of the current in terms of mode amplitudes

From (29), the calculation of the current is reduced to find an expression for $\partial \mathcal{P}_{0,0,0}^\pm / \partial q$. However, this is not a trivial task, because the term proportional to $\partial / \partial q$ in (17) vanishes for $k = 0$.

To proceed, we focus in (17) on $\omega = k = 0$, and for small q Taylor expand the dependency on q,

$$
\mathcal{P}_{0,0,q}^\pm = \mathcal{P}_{0,0,0}^\pm + q \frac{\partial \mathcal{P}_{0,0,0}^\pm}{\partial q} + \frac{q^2}{2} \frac{\partial^2 \mathcal{P}_{0,0,0}^\pm}{\partial q^2} + \cdots \tag{37}
$$

After summing the $-$ and $+$ forms of Eq. (17) for $\omega = k = 0$ and inserting expansion (37), we find, in each order, with n a non-negative integer,

$$
\begin{aligned}
0 &= \sum_n \left(\mathcal{F}_{n'}^{(0)+} \mathcal{P}_{0,-n'k_0,0}^+ + \mathcal{F}_{n'}^{(0)-} \mathcal{P}_{0,-n'k_0,0}^- \right) \\
&\quad + \sum_{l,m} \left(\mathcal{F}_{l,m}^{p+} \mathcal{P}_{-l\delta_p, -mk_0, 0}^+ + \mathcal{F}_{l,m}^{p-} \mathcal{P}_{-l\delta_p, -mk_0, q}^- \right),
\end{aligned} \tag{38}
$$

and

$$
\begin{aligned}
&\frac{(n+1)D_0}{i\hbar} \left(\frac{\partial^n \mathcal{P}_{0,0,0}^+}{\partial q^n} + \frac{\partial^n \mathcal{P}_{0,0,0}^-}{\partial q^n} \right) \\
&= \sum_{n'} \left(\mathcal{F}_{n'}^{(0)+} \frac{\partial^{n+1} \mathcal{P}_{0,-n'k_0,0}^+}{\partial q^{n+1}} + \mathcal{F}_{n'}^{(0)-} \frac{\partial^{n+1} \mathcal{P}_{0,-n'k_0,0}^-}{\partial q^{n+1}} \right) \\
&\quad + \sum_{l,m} \left(\mathcal{F}_{l,m}^{p+} \frac{\partial^{n+1} \mathcal{P}_{-l\delta_p, -mk_0, 0}^+}{\partial q^{n+1}} + \mathcal{F}_{l,m}^{p-} \frac{\partial^{n+1} \mathcal{P}_{-l\delta_p, -mk_0, 0}^-}{\partial q^{n+1}} \right).
\end{aligned} \tag{39}
$$

Equation (39) with $n = 1$ facilitates the task to calculate the current, because, by means of (29), it provides a useful expression in terms of derivatives with respect to q of amplitudes with either $k \neq 0$ or $\omega \neq 0$. These derivatives can be calculated by using the following equations, obtained by using the Taylor expansion:

$$
\frac{\partial^{n'} \mathcal{P}_{\omega,k,q}^\pm}{\partial q^{n'}} = \frac{\partial^{n'} \mathcal{P}_{\omega,k,0}^\pm}{\partial q^{n'}} + q \frac{\partial^{1+n'} \mathcal{P}_{\omega,k,0}^\pm}{\partial q^{1+n'}} + \frac{q^2}{2} \frac{\partial^{2+n'} \mathcal{P}_{\omega,k,0}^\pm}{\partial q^{2+n'}} + \cdots \tag{40}
$$

with n' a non-negative integer, in (17),

$$
\begin{aligned}
&\frac{\hbar k}{m_a} \frac{\partial \mathcal{P}_{\omega,k,0}^\pm}{\partial q} \\
&= i\omega \mathcal{P}_{\omega,k,0}^\pm + \sum_n \left(\gamma_n^\pm \mathcal{P}_{\omega,k-nk_0,0}^\pm - \gamma_n^\mp \mathcal{P}_{\omega,k-nk_0,0}^\mp \right), \tag{41}
\end{aligned}
$$

$$
\begin{aligned}
\frac{\hbar k}{m_a} \frac{\partial^2 \mathcal{P}_{\omega,k,0}^\pm}{\partial q^2} &= i\omega \frac{\partial \mathcal{P}_{\omega,k,0}^\pm}{\partial q} - \frac{i}{\hbar} \sum_n \mathcal{F}_n^{(0)\pm} \mathcal{P}_{\omega,k-nk_0,0}^\pm \\
&\quad - \frac{i}{\hbar} \sum_{l,m} \mathcal{F}_{l,m}^{p\pm} \mathcal{P}_{\omega-l\delta_p, k-mk_0, 0}^\pm \\
&\quad + \sum_n \left(\gamma_n^\pm \frac{\partial \mathcal{P}_{\omega,k-nk_0,0}^\pm}{\partial q} - \gamma_n^\mp \frac{\partial \mathcal{P}_{\omega,k-nk_0,0}^\mp}{\partial q} \right).
\end{aligned} \tag{42}
$$

The direct use of (41)–(42) allows us to calculate most terms, except the case $\partial \mathcal{P}^{\mp}_{\omega,0,0}/\partial q$ with $\omega \neq 0$. In this latter case, the first derivatives can still be found from (42), but requires

inversion of a 2×2 matrix, because both first derivative terms also appear on the right-hand side of the equation. Performing that calculation we obtain

$$
\frac{\partial \mathcal{P}^{\pm}_{\omega,0,0}}{\partial q} = \frac{1}{2\gamma_0 i\omega - \omega^2} \left[\frac{\gamma_0 i}{\hbar} \left[\sum_n \left(\mathcal{F}^{(0)+}_n \mathcal{P}^+_{\omega,-nk_0,0} + \mathcal{F}^{(0)-}_n \mathcal{P}^-_{\omega,-nk_0,0} \right) + \sum_{l,m} \left(\mathcal{F}^{p+}_{l,m} \mathcal{P}^+_{\omega-l\delta_p,-mk_0,0} + \mathcal{F}^{p-}_{l,m} \mathcal{P}^-_{\omega-l\delta_p,-mk_0,0} \right) \right] \right.
$$

$$
\left. - \frac{\omega}{\hbar} \left[\sum_n \mathcal{F}^{(0)\pm}_n \mathcal{P}^{\pm}_{\omega,k-nk_0,0} + \sum_{l,m} \mathcal{F}^{p\pm}_{l,m} \mathcal{P}^{\pm}_{\omega-l\delta_p,k-mk_0,0} \right] - i\omega \sum_{n\neq 0} \left(\gamma^{\pm}_n \frac{\partial \mathcal{P}^{\pm}_{\omega,-nk_0,0}}{\partial q} - \gamma^{\mp}_n \frac{\partial \mathcal{P}^{\mp}_{\omega,-nk_0,0}}{\partial q} \right) \right].
$$

$$(43)$$

It is then straightforward to arrive at an explicit expression for the current $\langle v \rangle$ or an arbitrary moment $\langle v^n \rangle$ using similar steps, in the form (30). The application to a system with Sisyphus cooling, such as those presented in Sec. II, reveals the presence of the regime of infinity density, as discussed in Sec. V.

C. Calculation of the mode amplitudes in the computer simulation

Numerical solutions of Eq. (2) are obtained by generating a large number of individual atomic trajectories [22] using a stochastic algorithm [33]. At a particular time, the atom is in a definite state $+$ or $-$.

For convenience, let us denote the atomic mode amplitudes for $q = 0$ as

$$
P_{\pm}[l, n] = \mathcal{P}^{\pm}_{l\delta_p, nk_0, 0}. \tag{44}
$$

They are the Fourier transform of the atomic density $P_{\pm}(x, t)$,

$$
P_{\pm}[l, n] = \frac{\delta_p}{2\pi} \int_0^{2\pi/\delta_p} dt \, e^{-il\delta_p t} \int dx \, e^{ink_0 x} P_{\pm}(x, t).
$$

$$
= \lim_{l' \to \infty} \frac{\delta_p}{2\pi l'} \int_0^{2\pi l'/\delta_p} dt \, e^{-il\delta_p t} \int dx \, e^{ink_0 x} P_{\pm}(x, t).
$$

$$(45)$$

The atomic density can be expressed in terms of atomic trajectories $x_j(\sigma_j(t), t)$, where $\sigma_j(t) = +1$ or -1 is the occupied state at time t in that trajectory, using the Dirac delta function and the Kronecker delta

$$
P_{\pm}(x, t) = \frac{1}{N} \sum_{j=1}^{N} \delta[x - x_j(\sigma_j(t), t)] \delta_{\sigma_j(t), \pm 1}. \tag{46}
$$

Thus, inserting (46) into (45) yields

$$
P_{\pm}[l, n] = \lim_{l' \to \infty} \frac{\delta_p}{2\pi l' N} \sum_{j=1}^{N} \int_0^{2\pi l'/\delta_p} dt
$$

$$
\times e^{i[nk_0 x_j(\sigma_j(t), t) - l\delta_p t]} \delta_{\sigma_j(t), \pm 1}. \tag{47}
$$

Since in the simulation individual atomic trajectories are generated, Eq. (47) can be readily implemented to compute the atomic mode coefficients, involving an average over many atomic trajectories and many probe periods.

IV. APPLICATION OF THE METHOD TO THE SYSTEM MODELS

Our goal is to express the current as (30), i.e., as a summation of terms proportional to the atomic mode amplitudes $P_{\pm}[l, n]$, with explicit analytical expressions for the intermediate coefficients $v^{\pm}_{n,l}$. In the 1D lin $\perp$ lin system, the force and rate constants (18) and (20), defining the optical potential (1) and transition rates (6), respectively, are given by

$$
\mathcal{F}^{(0)+}_{\pm 1} = \mp \frac{F_0}{2i}, \quad \mathcal{F}^{(0)-}_{\pm 1} = -\mathcal{F}^{(0)+}_{\pm 1} \tag{48}
$$

$$
\gamma^{\pm}_{\pm 0} = g_0, \quad \gamma^+_{\pm 1} = \frac{g_1}{2}, \quad \gamma^-_{\pm 1} = -\gamma^+_{\pm 1}. \tag{49}
$$

with $F_0 = k_0 U_0/2$.

In the 3D lin $\perp$ lin system, Eqs. (9)–(10), in addition to (48)–(49), there are the following coefficients:

$$
\mathcal{F}^{(0)+}_{\pm 2} = \pm \frac{F_0}{2i}, \quad \mathcal{F}^{(0)-}_{\pm 2} = \mathcal{F}^{(0)+}_{\pm 2} \tag{50}
$$

$$
\gamma^+_{\pm 2} = \frac{g_2}{2}, \quad \gamma^-_{\pm 2} = \gamma^+_{\pm 2}. \tag{51}
$$

In both cases, the addition of the probe to the potential has the same form, and the driving force coefficients (19) are given by

$$
\mathcal{F}^{p\pm}_{1,1} = -\frac{F_p e^{-i\phi_p}}{2i}, \quad \mathcal{F}^{p\pm}_{-1,-1} = \frac{F_p e^{+i\phi_p}}{2i}, \tag{52}
$$

where $F_p = U_0 \varepsilon_p k_0/2$.

It can be checked that the solution, of both systems, possesses the following atomic state symmetry:

$$
\mathcal{P}^-_{l\delta_p, nk_0, q} = (-1)^{n-l} \mathcal{P}^+_{l\delta_p, nk_0, q}. \tag{53}
$$

The proof involves verifying that (53) provides indeed a valid solution of (17), because of the specific way the sign of each term is changed in each atomic state, and invoking the uniqueness of the solution. This general, simple relation for the mode amplitudes $\mathcal{P}^-$ in terms of the coefficients in the other state, $\mathcal{P}^+$ allows us to focus only on the densities of one atomic sublevel.

A. 1D lin ⊥ lin system

By following the steps presented in Sec. III B, we obtain a summation of the current in terms of mode amplitudes

$$
\langle v \rangle_{1D} = \frac{m_a}{m_a F_0 g_1 - 2D_0 k_0} \left[- \frac{\mathrm{Im}[P_+[0,1]] 8 F_0 g_0^2}{k_0} \right.
$$

$$
+ \frac{\mathrm{Im}[P_+[0,2]] F_0 (-4 g_0 g_1 + F_0 k_0 / m_a)}{k_0}
$$

$$
+ \frac{\mathrm{Im}[e^{i\phi_p} P_+[1,2]] 2 F_0 F_p}{m_a} + \frac{\mathrm{Im}[e^{i\phi_p} P_+[1,1]] 2 F_p \delta_p^2}{k_0}
$$

$$
\left. + \frac{\mathrm{Im}[e^{i2\phi_p} P_+[2,2]] F_p^2}{m_a} \right]. \tag{54}
$$

Note the only contribution that depends explicitly on the probe frequency δ_p is the Brillouin mode $(l,n) = (1,1)$, the same propagating mode as the probe potential, all other modes only explicitly depend on the optical potential force F_0, probe amplitude F_p, or transition rates g_0 and g_1.

All terms in (54) share a common denominator, $m_a F_0 g_1 - 2D_0 k_0$, which produces a singularity when it is zero. The consequences will be discussed in Sec. V.

The expression (54) is validated numerically in Fig. 1, where we depict the contribution of each mode, $v[l,n]$, after numerically calculating the mode amplitudes $P_+[l,n]$ in the simulations using (47). As a test, we also show the sum of all contributions and compare it with the current calculated directly from its definition (4), confirming the analytical calculation. in all simulations, units are defined such that $m_a = \hbar = k_l = 1$.

Previous research [23,24,29,30] focused on one propagating mode, the mode $(l,n) = (1,1)$, which travels at speed δ_p / k_0 and is obviously excited by the probe potential, having the same frequency and wave number. Here this mode is confirmed to provide the most important contribution to the current. However, other modes are also excited as illustrated in Fig. 1. The atomic mode $(1,2)$, which moves with a reduced phase velocity $\delta_p / (2k_0)$, also significantly contributes to the current, though producing current in the opposite direction.

FIG. 1. Current and mode contributions to the current as a function of the probe amplitude ε_p for the 1D lin ⊥ lin system under a probe perturbation propagating to the right (7). Each mode (l,n) has a frequency $\omega = l\delta_p$ and wave number $k = nk_0$. Mode amplitudes are measured in the simulation via (47), and their precise contribution to the current determined using (54), taking averages over 1.5×10^6 trajectories. Units are defined such that $m_a = \hbar = k_l = 1$. Here $U_0 = 50$ and $\Gamma' = 7.5$, $\delta_p = 10$, and $\phi_p = -\pi/2$. The dashed line is the sum of all current contributions, and the filled diamonds are the current calculated from its definition (4). From top to bottom, the blue, black, green, red, and orange solid lines denote the contributions $v[1,1]$ $v[0,1]$, $v[2,2]$, $v[0,2]$, $v[1,2]$, respectively.

The nonpropagating mode $(0,2)$ is also observed to produce contributions to the current in the opposite direction.

B. 3D lin ⊥ lin system

When compared with the 1D lin ⊥ lin system, in the 3D lin ⊥ lin system the additional terms (50)–(51) produce new terms in the summation making up the average velocity, both new contributing terms appearing for the previously discussed modes, and new contributions from other modes,

$$
\langle v \rangle_{3D} = \frac{m_a}{m_a F_0 g_1 - 2D_0 k_0} \left[- \frac{\mathrm{Im}[P_+[0,1]] F_0 \left(8 g_0^2 - 4 g_2^2/3 + F_0 k_0/(2m_a) \right)}{k_0} + \frac{\mathrm{Im}[P_+[0,2]] F_0 (-4 g_0 g_1 - 8 g_1 g_2/3 + F_0 k_0/m_a)}{k_0} \right.
$$

$$
+ \frac{\mathrm{Im}[P_+[0,3]] F_0 \left(-16 g_0 g_1/3 - 2 g_2^2 - 3 F_0 k_0/(2m_a) \right)}{k_0} + \frac{\mathrm{Im}[P_+[0,4]] F_0 (-2 g_1 g_2/3 + F_0 k_0/(2m_a))}{k_0}
$$

$$
- \frac{\mathrm{Im}[P_+[0,5]] F_0 2 g_2^2}{3 k_0} + \frac{\mathrm{Im}[e^{i\phi_p} P_+[1,2]] 2 F_0 F_p}{m_a} + \frac{\mathrm{Im}[e^{i\phi_p} P_+[1,-1]] F_0 F_p}{2 m_a}
$$

$$
\left. - \frac{\mathrm{Im}[e^{i\phi_p} P_+[1,3]] 3 F_0 F_p}{2 m_a} + \frac{\mathrm{Im}[e^{i\phi_p} P_+[1,1]] 2 F_p \delta_p^2}{k_0} + \frac{\mathrm{Im}[e^{i2\phi_p} P_+[2,2]] F_p^2}{m_a} \right]. \tag{55}
$$

Figure 2 shows the numerical results in the 3D lin ⊥ lin system. Like in the previous one, the biggest contributor to the current is the propagating mode $(1,1)$, which produces movement in the same direction as the propagating probe potential. The nonpropagating mode $(0,1)$ also produces a contribution
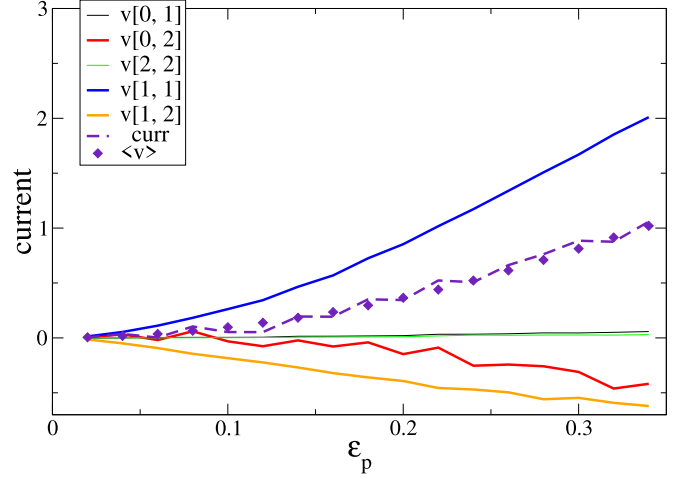
comparable to that of the mode $(1,1)$. New contributions from the nonpropagating modes $(0,3)$, $(0,4)$ and $(0,5)$—due to the extra mode-connecting terms in (9) and (10)—are observed, all producing current in the opposite direction of propagation. A similar feature is observed in the new mode $(1,3)$, which
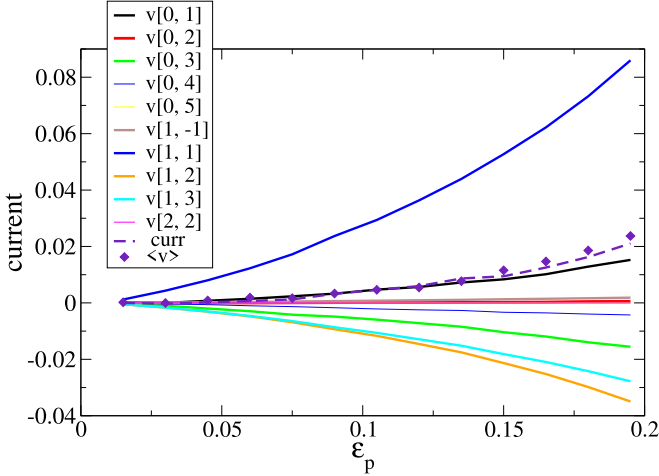
FIG. 2. Current and mode contributions to the current as a function of the probe amplitude ε_p for a 3D lin $\perp$ lin system under a probe perturbation propagating to the right in the x direction (9), with $U_0 = 200$, $\Gamma' = 2.85$, $\theta_x = \theta_y = 25$, $\delta_p = 12$, and $\phi_p = \pi$—values matching the experiment in [25]. The dashed line is the sum of all current contributions, and the filled diamonds is the current measured directly in the simulation. From top to bottom, the blue, black, brown, red, thin blue, green, cyan, and orange solid lines denote the contributions $v[1, 1]$, $v[0, 1]$, $v[1, -1]$, $v[0, 2]$, $v[0, 4]$, $v[0, 3]$, $v[1, 3]$, and $v[1, 2]$, respectively ($v[0, 5]$ is almost zero, and thus not appreciable).

similarly to the propagating mode $(1,2)$, produces current in the opposite direction. On the other hand, the mode $(1, -1)$ is observed to produce a very small contribution to the current in the direction of propagation of the probe potential. The contributions of the modes $(0,5)$ and $(2,2)$ are so small they cannot be seen in Fig. 2. The overall current is much smaller, about four times smaller, than the one produced alone by the Brillouin mode $(1,1)$.

V. INTO THE REGIME OF INFINITE DENSITY

Note the optical potential force $\mathcal{F}_{\pm 1}^{(0)\pm}$, Eq. (48), inverts its sign when the atomic state is changed. This fact is crucially coupled to the state-alternating sign in the transition rate $\gamma_{\pm 1}^{\pm}$, Eq. (49). This is responsible for the celebrated Sisyphus cooling, that is, for the dissipative mechanism resulting from the transitions taking place with higher probability when the atoms are at the top of the optical potential barriers. As the atoms move around the potential wells, random kicks resulting from the interaction with circularly polarized photons increase their kinetic energy, which is then lost in the transition. As a result, the atoms are spending most of the time climbing hills, like the punishment inflicted on the king Sisyphus of ancient Greek mythology. But this requires the concerted action of the potential and the transition rates, as the position of potential barriers must be changing accordingly to the rate's maxima in each transition.

However, it is known the potential should not be too shallow [27], or the dynamics may yield non-normalizable probability densities [17,19], which is known to exhibit superdiffusion [8]. Indeed, the calculations presented in Sec. IV

indicate that the current diverges to infinity, in both studied systems, when

$$F_0 g_1 - 2D_0 k_0 / m_a = 0, \qquad (56)$$

It is a consequence of the appearance of a term proportional to $\partial \mathcal{P}_{0,0,0}^+ / \partial q + \partial \mathcal{P}_{0,0,0}^- / \partial q$ on the right-hand side of Eq. (39) (with $n = 1$), after the substitutions (41)–(42) are applied. Those terms have to be taken to the left-hand side in order to complete the calculation.

In fact, a similar singularity happens in any moment $\langle v^n \rangle$. Using (31) and (39), and looking for the terms on the right-hand side that yield a contribution containing $\partial^n \mathcal{P}_{0,0,0}^+ / \partial q^n + \partial^n \mathcal{P}_{0,0,0}^- / \partial q^n$, i.e., the terms proportional to $\mathcal{F}_{+1}^{(0)\pm} \gamma_{-1}^{\pm}$ and $\mathcal{F}_{-1}^{(0)\pm} \gamma_{+1}^{\pm}$, yields the common factor, $[1 - F_0 g_1 m_a / (D_0 k_0 (n + 1))]^{-1}$, and thus the following singularity condition,

$$F_0 g_1 - (1 + n) D_0 k_0 / m_a = 0, \qquad (57)$$

which in terms of the potential depth is written as

$$U_0 = \frac{2(1 + n) D_0}{g_1 m_a}. \qquad (58)$$

Though this result has been obtained from the semiclassical equations (2), which do not explicitly contain all the diffusive terms predicted by the semiclassical derivation, that is, the terms $\partial^2 D_{\mp\pm} P_{\mp} / \partial p^2$ and the spatial dependence of the noise coefficient, performing the calculation in the more complex system model shows that the exact same result (57) is obtained if one considers D_0 as the spatial average of all diffusive terms.

This singularity can be identified with the threshold for the transition into an anomalous regime, in which the n moment of the velocity distribution, $\langle v(t)^n \rangle$, diverges for long times. The result (58) is in perfect agreement with the prediction [18,19] for the system 1D lin $\perp$ lin obtained from a simplified, approximate Fokker-Planck equation [27] for shallow lattices, when the noise strength D_0 contains the spatial average of both diffusive terms $D_{\mp\pm}$ and $D_{\pm\pm}$ [22], i.e., $D_0 = (35 + 6)\hbar^2 k_l^2 \Gamma' / 90$. This is remarkable, as our method uses the full semiclassical equations (2), and hence, unlike the approximate Fokker-Planck equation, it does explicitly take into account the microscopic origin of Sisyphus cooling, including the periodicity of the lattice potential and transitions between the atomic sublevels.

The only assumption made by the method presented here is the existence of the Taylor expansion (40), which is numerically confirmed by the simulations presented in the paper in the regime above the singularity. In contrast, in shallow lattices, i.e., with potential wells U_0 below the threshold given by (58), this assumption does not hold, giving rise to the regime of infinite densities, with diverging moments and non-normalizable densities. In the 3D lin $\perp$ lin system, to accurately cover the shallow potential regime, D_0 should also include the spatial average the diffusive term $D_{\mp\pm}$, thus $D_0 = (1 + 1/5)5\hbar^2 k_0^2 \Gamma' / 18$.

VI. CONCLUSIONS

Starting from the semiclassical equations for the atomic phase-space densities, we have presented an exact method to

calculate the contribution to the current of the excited atomic density waves in cold atoms undergoing Sisyphus cooling. Explicit analytical expressions are provided for the 1D lin ⊥ lin system under a simple symmetry-breaking perturbation, as well as the one-dimensional model that results from focusing on a specific direction in the 3D lin ⊥ lin system.

The analytical results are validated with numerical simulations of the stochastic atomic trajectories associated with the semiclassical equations. They show that several atomic modes, not just the one associated with the perturbation, contribute relevantly to the directed motion, with most of them doing so in the opposite direction of propagation than that of the applied perturbation.

Additionally, the analytical solution predicts a singularity for each moment of the velocity distribution, which is identified with the threshold for the transition to the regime of infinite density. The threshold values of the present work are identical to the ones obtained [18,19] from an approximated Fokker-Planck equation of the semiclassical equations, derived by spatial and Zeeman level averaging the latter, in the 1D lin ⊥ lin system, thus providing a solid ground to previous analytical results. Finally, it is worth mentioning that the proposed method can easily be applied to more complex systems and driving perturbations.

[1] F. Schreck and K. van Druten, Laser cooling for quantum gases, Nat. Phys. **17**, 1296 (2021).

[2] G. Grynberg and C. Robilliard, Cold atoms in dissipative optical lattices, Phys. Rep. **355**, 335 (2001).

[3] C. Mennerat-Robilliard, D. Lucas, S. Guibal, J. Tabosa, C. Jurczak, J.-Y. Courtois, and G. Grynberg, Ratchet for Cold Rubidium Atoms: The Asymmetric Optical Lattice, Phys. Rev. Lett. **82**, 851 (1999).

[4] M. Schiavoni, L. Sanchez-Palencia, F. Renzoni, and G. Grynberg, Phase Control of Directed Diffusion in a Symmetric Optical Lattice, Phys. Rev. Lett. **90**, 094101 (2003).

[5] R. Gommers, S. Bergamini, and F. Renzoni, Dissipation-Induced Symmetry Breaking in a Driven Optical Lattice, Phys. Rev. Lett. **95**, 073003 (2005).

[6] R. Gommers, S. Denisov, and F. Renzoni, Quasiperiodically Driven Ratchets for Cold Atoms, Phys. Rev. Lett. **96**, 240604 (2006).

[7] P. H. Jones, M. Goonasekera, D. R. Meacher, T. Jonckheere, and T. S. Monteiro, Directed Motion for Delta-Kicked Atoms with Broken Symmetries: Comparison between Theory and Experiment, Phys. Rev. Lett. **98**, 073002 (2007).

[8] A. Wickenbrock, P. C. Holz, N. A. Wahab, P. Phoonthong, D. Cubero, and F. Renzoni, Vibrational Mechanics in an Optical Lattice: Controlling Transport via Potential Renormalization, Phys. Rev. Lett. **108**, 020603 (2012).

[9] T. Salger, S. Kling, T. Hecking, C. Geckeler, L. Morales-Molina, and M. Weitz, Directed transport of atoms in a Hamiltonian quantum Ratchet, Science **326**, 1241 (2009).

[10] C. Grossert, M. Leder, S. Denisov, P. Hänggi, and M. Weitz, Experimental control of transport resonances in a coherent quantum rocking Ratchet, Nat. Commun. **7**, 10440 (2016).

[11] P. Hänggi and F. Marchesoni, Artificial Brownian motors: Controlling transport on the nanoscale, Rev. Mod. Phys. **81**, 387 (2009).

[12] D. Cubero and F. Renzoni, *Brownian Ratchets: From Statistical Physics to Bio and Nano-motors* (Cambridge University Press, Cambridge, 2016).

[13] P. Reimann, M. Grifoni, and P. Hänggi, Quantum Ratchets, Phys. Rev. Lett. **79**, 10 (1997).

[14] J. B. Majer, J. Peguiron, M. Grifoni, M. Tusveld, and J. E. Mooij, Quantum Ratchet Effect for Vortices, Phys. Rev. Lett. **90**, 056802 (2003).

[15] I. Zapata, S. Albaladejo, J. M. R. Parrondo, J. J. Saenz, and F. Sols, Deterministic Ratchet from Stationary Light Fields, Phys. Rev. Lett. **103**, 130601 (2009).

[16] G. Lyu and G. Watanabe, Persistent current by a static non-Hermitian Ratchet, Phys. Rev. A **105**, 023328 (2022).

[17] E. Lutz and F. Renzoni, Beyond Boltzmann-Gibbs statistical mechanics in optical lattices, Nat. Phys. **9**, 615 (2013).

[18] D. A. Kessler and E. Barkai, Infinite Covariant Density for Diffusion in Logarithmic Potentials and Optical Lattices, Phys. Rev. Lett. **105**, 120602 (2010).

[19] P.C. Holz, A. Dechant, and E. Lutz, Infinite density for cold atoms in shallow optical lattices, Europhys. Lett. **109**, 23001 (2015).

[20] E. Barkai, G. Radons, and T. Akimoto, Transitions in the Ergodicity of Subrecoil-Laser-Cooled Gases, Phys. Rev. Lett. **127**, 140605 (2021).

[21] T. Akimoto, E. Barkai, and G. Radons, Infinite ergodic theory for three heterogeneous stochastic models with application to subrecoil laser cooling, Phys. Rev. E **105**, 064126 (2022).

[22] K. Petsas, G. Grynberg, and J.-Y. Courtois, Semiclassical Monte Carlo approaches for realistic atoms in optical lattices, Eur. Phys. J. D **6**, 29 (1999).

[23] J. Y. Courtois, S. Guibal, D. R. Meacher, P. Verkerk, and G. Grynberg, Propagating Elementary Excitation in a Dilute Optical Lattice, Phys. Rev. Lett. **77**, 40 (1996).

[24] L. Sanchez-Palencia, F.-R. Carminati, M. Schiavoni, F. Renzoni, and G. Grynberg, Brillouin Propagation Modes in Optical Lattices: Interpretation in Terms of Nonconventional Stochastic Resonance, Phys. Rev. Lett. **88**, 133903 (2002).

[25] A. Staron, K. Jiang, C. Scoggins, D. Wingert, D. Cubero, and S. Bali, Observation of stochastic resonance in directed propagation of cold atoms, Phys. Rev. Res. **4**, 043211 (2022).

[26] M. Borromeo and F. Marchesoni, Artificial Sieves for Quasimassless Particles, Phys. Rev. Lett. **99**, 150605 (2007).

[27] Y. Castin, J. Dalibard, and C. Cohen.Tannoudji, *Light Induced Kinetic Effects on Atoms, Ions and Molecules* (ETS Editrice, Pisa, 1991) Chap. The limits of Sisyphus cooling, pp. 5–24.

[28] F. Renzoni, Driven Ratchets for cold atoms, Adv. At. Mol. Opt. Phys. **57**, 1 (2009).

[29] M. Schiavoni, F.-R. Carminati, L. Sanchez-Palencia, F. Renzoni, and G. Grynberg, Stochastic resonance in periodic

potentials: Realization in a dissipative optical lattice, Europhys. Lett. **59**, 493 (2002).

[30] F.-R. Carminati, M. Schiavoni, Y. Todorov, F. Renzoni, and G. Grynberg, Pump-probe spectroscopy of atoms cooled in a 3d lin-perp-lin optical lattice, Eur. Phys. J. D **22**, 311 (2003).

[31] L. Sanchez-Palencia and G. Grynberg, Synchronization of Hamiltonian motion and dissipative effects in optical lattices:

Evidence for a stochastic resonance, Phys. Rev. A **68**, 023404 (2003).

[32] D. Cubero and F. Renzoni, Hidden Symmetries, Instabilities, and Current Suppression in Brownian Ratchets, Phys. Rev. Lett. **116**, 010602 (2016).

[33] P. E. Kloeden and E. Platen, *Numerical Solution of Stochastic Differential Equations* (Springer, New York, 1992).